

Review

Structural and Electronic Properties of Polyoxovanadoborates Containing the $[V_{12}B_{18}O_{60}]$ Core in Different Mixed Valence States

Patricio Hermosilla-Ibáñez ^{1,2}, Karina Muñoz-Becerra ^{1,2}, Verónica Paredes-García ^{2,3}, Eric Le Fur ⁴, Evgenia Spodine ^{2,5,*} and Diego Venegas-Yazigi ^{1,2,*}

¹ Facultad de Química y Biología, Universidad de Santiago de Chile, USACH; Av. Libertador Bernardo O'Higgins 3363, 9170022, Santiago, Chile; E-Mails: patricio.hermosilla@usach.cl (P.H.-I.); karina.munozbe@usach.cl (K.M.-B.); diego.venegas@usach.cl (D.V.-Y.)

² Centro para el Desarrollo de la Nanociencia y Nanotecnología, CEDENNA, 9170022, Santiago, Chile

³ Departamento de Ciencias Químicas, Universidad Andres Bello, Republica 275, 8370146, Santiago, Chile; E-Mail: vparedes@unab.cl

⁴ ENSCR, UMR 6226, 11, allée de Beaulieu - CS 50837-35708 Rennes Cedex 07, France; E-Mail: eric.le-fur@ensc-rennes.fr

⁵ Facultad de Ciencias Químicas y Farmacéuticas, Universidad de Chile; Sergio Livingstone 1007, Independencia, 8380492, Santiago, Chile; E-Mail: espodine@ciq.uchile.cl

* Authors to whom correspondence should be addressed; E-Mails: espodine@ciq.uchile.cl (E.S.); diego.venegas@usach.cl (D.V.-Y.); Tel.: +56-2-2718-1079 (D.V.-Y.); Fax: +56-2-2681-2108 (D.V.-Y.).

Academic Editors: Greta Ricarda Patzke and Pierre-Emmanuel Car

Received: 15 April 2015 / Accepted: 5 June 2015 / Published: 3 July 2015

Abstract: This review summarizes all published data until April 2015 related to crystalline lattices formed by the $[V_{12}B_{18}O_{60}]$ core, which generates polyanionic clusters with different degrees of protonation and mixed-valence ratios. The negative charge of this cluster is counterbalanced by different cations such as protonated amines, hydronium, and alkaline, and transition metal ions. The cluster is shown to form extended 1D, 2D, or 3D frameworks by forming covalent bonds or presenting hydrogen bond interactions with the present secondary cations. These cations have little influence on the solid state reflectance UV-visible spectra of the polyanionic cluster, but are shown to modify the FT-IR spectra and the magnetic behavior of the different reported species.

Keywords: $[V_{12}B_{18}O_{60}]$; polyoxovanadoborate; VBO; electronic properties; FT-IR; reflectance UV-vis; magnetic behavior

1. Introduction

Polyoxometalates (POMs) have been systematically studied during the last decades due to their structural variety and physico-chemical properties [1–13]. The structural variety of these polyanionic clusters is generated by their interaction with or bonding to different cationic species such as protonated amines, ammonium and hydronium ions, alkaline, transition metal, and lanthanide ions. These cationic species can exist in the lattice as charge-compensating agents, or linked to the external oxygen atoms of the polyanionic species, and thus serve to increase the dimensionality of these systems [14–19]. The crystalline packing is stabilized by hydrogen bonds, in the case of ammonium cations, or by the formation of covalent bonds through the interaction of the external oxygen atoms of the polyanionic species with different metal cations, such as alkaline or transition metal ions.

The polyoxovanadates (VO) constitute an appealing family of polyanions, due principally to the structural plasticity that vanadium atoms present in their different oxidation states. The variable topology of the polynuclear VO systems is given by the $\{V_xO_y\}$ entities with diverse connectivities. The literature reports polyoxovanadates containing from five to 34 metal centers: $[V_5O_{14}]^{3-}$ [20], $[V_{10}O_{28}]^{6-}$ [21], $[V_{12}O_{32}]^{4-}$ [22], $[V_{13}O_{34}]^{3-}$ [23], $[V_{15}O_{42}]^{9-}$ [24], $[V_{15}O_{36}]^{5-}$ [25], $[V_{18}O_{42}]^{12-}$ [26], $[V_{19}O_{49}]^{9-}$ [27], $[V_{22}O_{54}]^{6-}$ [28], and $[V_{34}O_{82}]^{10-}$ [29]. When a heteroatom such as boron is condensed in these systems, the structural richness of the VO cluster is increased; this new family of polyoxometalates is termed polyoxovanadoborates (VBO). To date the known polyanions included in the VBO family are $[V_6B_{20}]$ [30–33], $[V_6B_{22}]$ [34], $[V_{10}B_{28}]$ [35–37], $[V_{12}B_{16}]$ [38–41], $[V_{12}B_{17}]$ [42], $[V_{12}B_{18}]$ [31,39–59], and $[V_{12}B_{32}]$ [60,61]. The first VBO polyanions were reported at the end of the 1990s by Rijssenbeek *et al.* [42], and in 2000 Williams *et al.* published the first review on vanadoborate clusters as a chapter in *Contemporary Boron Chemistry* [62].

As a result of V^V and V^{IV} sharing similar geometries, the redox processes between both states can be accessed by keeping the initial structure of the polyanion constant, thus generating several mixed valence systems. This feature is directly related to the magnetic and electronic properties shown by these compounds. However, these properties have been studied less extensively than the structural ones. In this review we report and discuss the structural and electronic properties of several polyanions derived from the $[V_{12}B_{18}O_{60}]$ core and their corresponding crystalline lattices.

2. Polyoxovanadoborates: Vanadate and Borate Fragments

The structures of all the VBO compounds reported in the literature are formed by the condensation of vanadate and borate fragments. The vanadate fragments always contain five-coordinated vanadium atoms (VO_5) in a [4+1] square base pyramidal coordination geometry, while the borate fragments include trigonal (BO_3) and tetrahedral (BO_4) borate units. The different connectivity between the (VO_5), (BO_3), and (BO_4) units leads to varied VBO cores with open barrel-like structures ($[V_{10}B_{28}]$ and $[V_{12}B_{32}]$), and closed spherical-like structures ($[V_6B_{20}]$, $[V_6B_{22}]$, $[V_{12}B_{16}]$, $[V_{12}B_{17}]$, and $[V_{12}B_{18}]$). Among all the

abovementioned clusters, $[V_{12}B_{18}]$ is the one most studied from a structural point of view.

2.1. Vanadate Fragments

Some selected examples of clusters have been analyzed in order to summarize the bond lengths given for the following fragments.

$[V_6O_{18}]$ -type A: The $[V_6O_{18}]$ -type A hexanuclear fragment shown in Figure 1a consists of six (VO_5) units connected by two equatorial oxygen atoms sharing two opposite edges to form a ring-like structure. In this moiety, the vanadium atoms are coplanar and the $V=O$ groups are on the periphery. This hexanuclear ring is found in the structures formed by the $[V_6B_{20}]$ and $[V_6B_{22}]$ cores. The $V=O$ bond lengths range from 1.605 to 1.625 Å, while the $V-O$ distances are between 1.944 and 1.970 Å [30,33].

$[V_6O_{18}]$ -type B: The topology of this fragment changes from the above mentioned hexanuclear ring to a triangular array (Figure 1b), due to the different condensation of the (VO_5) units, which are arranged in an alternated way of adjacent and opposite edges. This fragment can be found solely in the $[V_{12}B_{18}]$ core. The $V=O$ and $V-O$ bonds lengths range from 1.599 to 1.638 Å, and between 1.906 and 2.023 Å, respectively [43,52].

$[V_{10}O_{30}]$: This decanuclear moiety is similar to the $[V_6O_{18}]$ -type A, where the (VO_5) polyhedra share their opposite edges, forming a coplanar toroidal ring (Figure 1c). The compounds constituted by the $[V_{10}B_{28}]$ core present this fragment in their structures. The $V=O$ bond distances range from 1.599 to 1.640 Å; the $V-O$ bond distances range from 1.894 to 1.989 Å [35,63].

$[V_{12}O_{36}]$ -type A: This dodecanuclear vanadate fragment can be seen as the union of two mutually perpendicular semicircles, each one formed by five (VO_5) polyhedra linked by opposite edges. Both semicircles are connected by two additional (VO_5) polyhedral, thus forming a continuous ring as shown in Figure 1d. This moiety is found in the compounds containing the $[V_{12}B_{16}]$ and $[V_{12}B_{17}]$ cores. The $V=O$ bond distances are between 1.609 and 1.632 Å, while the $V-O$ bond distances range from 1.919 to 2.019 Å [40,41].

$[V_{12}O_{36}]$ -type B: This dodecanuclear fragment is described as a planar ring, whose topology is similar to the above-mentioned $[V_6O_{18}]$ -type A and $[V_{10}O_{30}]$ rings (Figure 1e). This fragment can be found in the structures of compounds with the $[V_{12}B_{32}]$ core. The $V=O$ and $V-O$ bonds lengths range from 1.569 to 1.649 Å, and between 1.890 and 1.990 Å, respectively [60,61].

As expected, the shorter distances are observed for the vanadyl groups ($V=O$), as compared to the single bonds ($V-O$). However, the analysis of the different vanadium-oxygen distances for all the vanadate fragments will depend on the mixed valence ratio, which is not the case for the borate fragments. Therefore a comparative analysis is not possible.

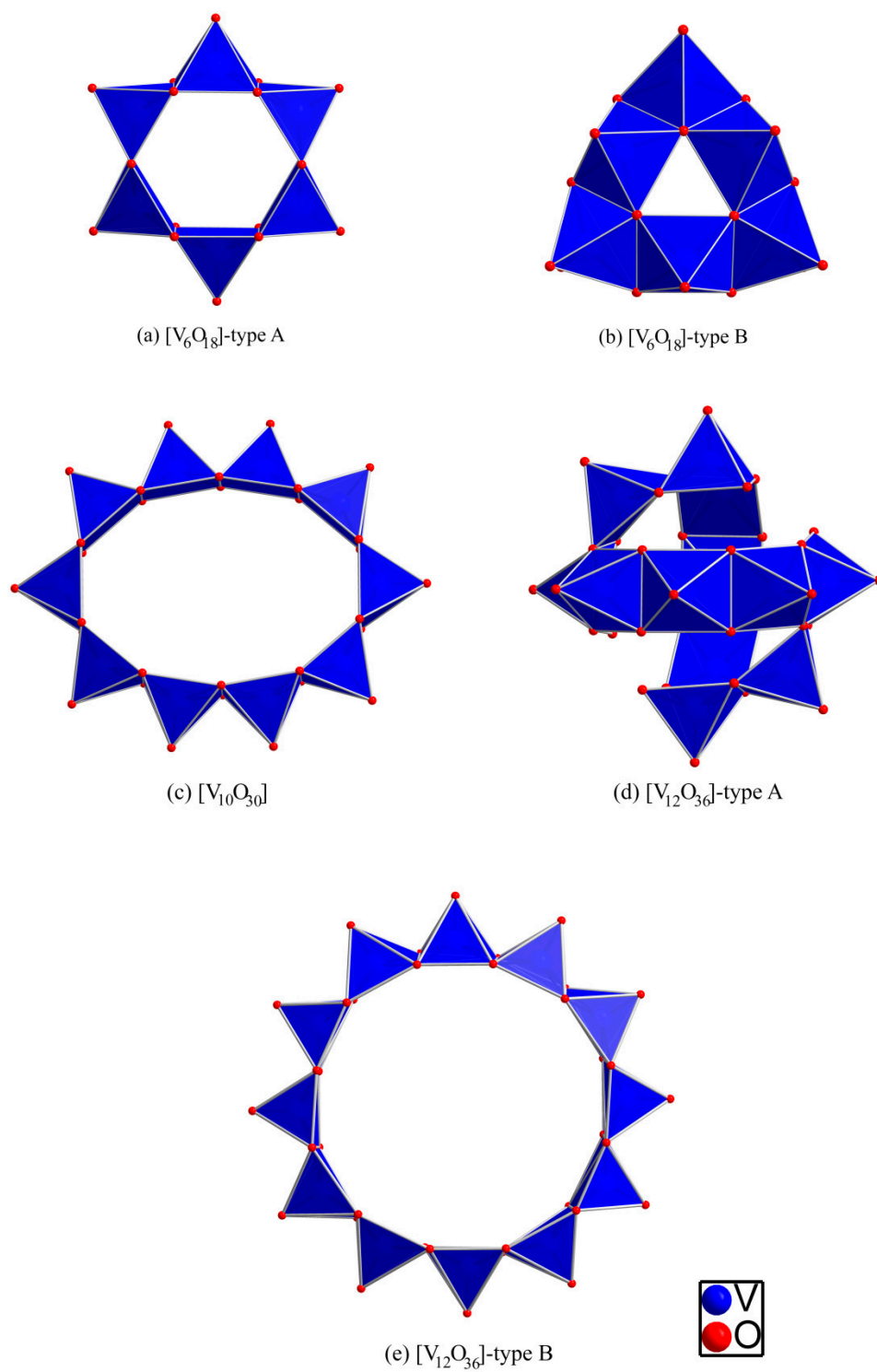


Figure 1. Polyhedral representation of the vanadate fragments.

2.2. Borate Fragments

In order to describe the different borate units, the topological classification proposed by Christ and Clark will be used [64]. Some selected examples of clusters have been considered in order to analyze the bond lengths given for the following fragments.

[B₁₀O₂₂]¹⁴⁻: This unit is composed by three (B₃O₈)⁷⁻ building-blocks connected to an additional (BO₄) entity, located in the middle of the fragment, as shown in Figure 2a. The triangular decaborate unit has three trigonal boron atoms at the corner of the triangle, and seven tetrahedral boron atoms 10[3: Δ+7T]. This decaborate is present in compounds with the [V₆B₂₀] core. The trigonal B-O bonds range from 1.349-1.391 Å, while the tetrahedral ones are between 1.425 and 1.545 Å [30,33].

[B₁₁O₂₄]¹⁵⁻: This undecaborate can be described as constituted by the abovementioned [B₁₀O₂₂]¹⁴⁻ fragment with an extra (BO₃) unit linked to the apical oxygen atom of the central tetrahedral (BO₄) group (Figure 2b) 11[4:Δ+7T]. This polyborate fragment has been described in compounds formed by the [V₆B₂₂] core. The trigonal and tetrahedral B-O bond distances range from 1.359 to 1.376 Å, and 1.430 to 1.546 Å, respectively [34].

[B₁₄O₃₂]²²⁻: The structure of this ring-like fragment is composed of eight tetrahedral and six trigonal boron atoms. Four (BO₄) units form two pairs and these are linked by two (BO₃) group forming a ring (Figure 2c); four additional (BO₃) entities are terminal groups bridging each pair of (BO₄) groups 14:2[2(3:Δ+2T)+(3:Δ)]. The compounds containing the [V₁₀B₂₈] core have this tetradecaborate unit. The B-O bond distances of the trigonal units range from 1.338 and 1.391 Å, while the B-O bond distances of the tetrahedral units are between 1.422 and 1.500 Å [35,63].

[B₈O₂₁]²¹⁻: This polyanionic entity is the lowest borate nuclearity fragment described to date. This structure is formed by a chain of six tetrahedral (BO₄) units. Two trigonal (BO₃) units bridge the second/third and fourth/fifth tetrahedral units of the chain (Figure 2d) 8:2[4:Δ+3T]. This fragment is found in clusters with the [V₁₂B₁₆] core. The B-O bond distances of the trigonal and tetrahedral units are between 1.348 and 1.389 Å, and 1.416 and 1.530 Å, respectively [40,41].

[B₁₈O₄₂]³⁰⁻: This polyborate ring forms part of the compounds containing the [V₁₂B₁₈] core. It is made of six (B₃O₇)⁵⁻ units, each one constituted by one trigonal and two tetrahedral boron atoms. Each (B₃O₇)⁵⁻ building-block contains one terminal (BO₃) group, and therefore each [B₁₈O₄₂]³⁰⁻ fragment has six peripheral (BO₃) units, 18[6: Δ+12T] (Figure 2e). The trigonal B-O bonds range from 1.340 to 1.382 Å, while the tetrahedral ones are between 1.420 and 1.525 Å [43,52].

[B₁₆O₃₆]²⁴⁻: This polyborate ring is formed of four pairs of (BO₄) units linked by four (BO₃) trigonal entities; each pair is additionally condensed to a terminal trigonal BO₃, 16[8:Δ+8T] (Figure 2f). This fragment is part of the [V₁₂B₃₂] family. The B-O bond distances are between 1.310 and 1.450 Å for the trigonal units, and between 1.410 and 1.530 Å for the tetrahedral units [60,61].

Based on the abovementioned data, it is possible to infer that all the trigonal B-O bond distances are shorter than those corresponding to the tetrahedral ones. An exception is that of the [B₁₆O₃₆]²⁴⁻ fragment, which has been reported in only two studies [60].

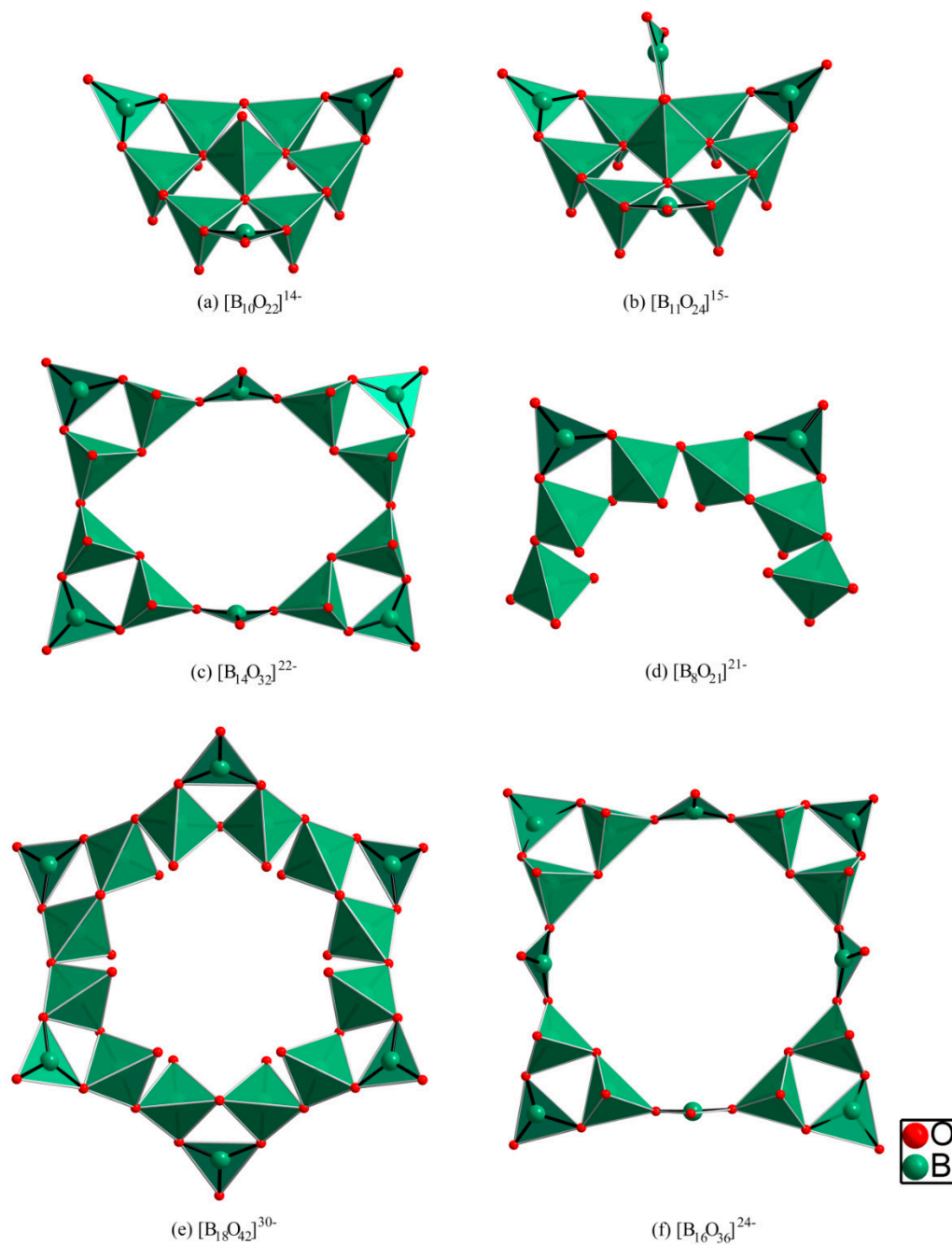


Figure 2. Polyhedral representation of the borate fragments.

Figure 3 shows the different polyoxovanadoborate clusters $[V_xB_yO_z]$ generated by the condensation of the $[V_iO_j]$ and $[B_hO_k]$ fragments described above.

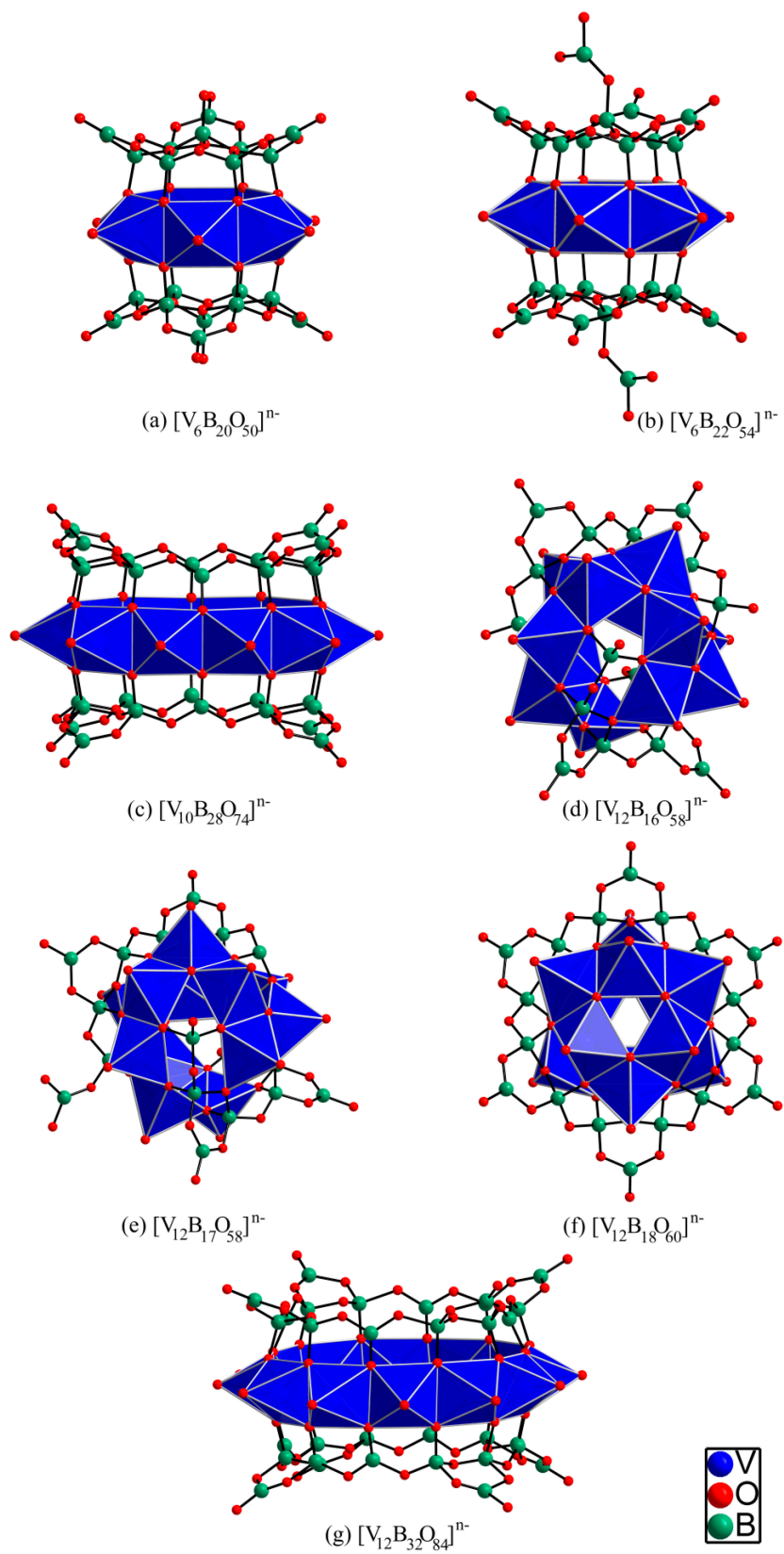


Figure 3. Structural representation of the different polyoxovanadoborate cores.

3. Structural Description of the $[V_{12}B_{18}O_{60}]$ Core

The $[V_{12}B_{18}O_{60}]$ polyoxovanadoborate core consists of two vanadate $[V_6O_{18}]$ -type B and one $[B_{18}O_{42}]^{30-}$ borate fragments. Each vanadate fragment has six five-coordinated (VO_5) vanadium centers adopting a $[4+1]$ square base pyramidal coordination geometry. The vanadium atom is displaced from the best mean plane formed by the four equatorial oxygen atoms towards the axial vanadyl group, by *ca.* 0.7 Å. The angles formed between the V=O bond and the four equatorial V-O bonds are from 100 to 110°. All the V=O distances are in the range of 1.57 Å to 1.68 Å [65]. The borate fragment $[B_{18}O_{42}]^{30-}$ is condensed to the two $[V_6O_{18}]$ -type B moieties, thus remaining in a sandwich-type configuration in the middle of the $[V_{12}B_{18}O_{60}]$ polyanion (Figure 3f). A water molecule is always found (with partial occupancy most of the time) within the cavity of the $[V_{12}B_{18}O_{60}]$ polyanion.

4. $[V_{12}B_{18}O_{60}]$ Cores with Protonated Amines as Counterbalancing Ions

In this section lattices based on the $[V_{12}B_{18}O_{60}]$ core including protonated diamines, ammonium, and hydronium as counterbalancing ions will be described, and are listed in Table 1. Rijssenbeek *et al.* [42], in 1997, obtained by hydrothermal synthesis the first two VBO crystalline systems based on the $[V_{12}B_{18}O_{60}]$ core, with 1,2-ethylenediammonium (enH_2)²⁺ (**1**) and 1,3-propanediammonium (1,3-diapH₂)²⁺ (**2**) ions to compensate for the negative charge. The authors mentioned that the organic molecule is included in the synthetic medium as a structure-directing agent of the framework. In both (**1**) and (**2**), the diammonium ions occupy the intercluster space along with water solvation molecules. In 2011 Liu *et al.* [49] reported another lattice having 1,2-propanediammonium (1,2-dapH₂)²⁺ or (H₂dap)²⁺ (**3**), along with hydronium ions as charge counterbalance cations. (**3**) was also obtained by hydrothermal synthesis including additionally Cu(CH₃COO)₂·2H₂O in the reaction mixture, a species that was not included in the final crystalline packing. However, the authors did not mention if the same lattice is formed leaving out the copper source. Bigger ammonium cations derived from triethylenetetramine (H₃teta)³⁺ together with hydronium ions were found in the crystalline system (**4**) based on the $[V_{12}B_{18}O_{60}]$ core, studied by Liu *et al.* in 2013 [34]. The hydrothermal synthetic procedure used also included a secondary metal source, metallic cobalt powder. In this case, the authors pointed out that the presence of the transition metal is indispensable to obtain (**4**). In 2014 we reported a new crystalline system (**5**) containing (1,3-diapH₂)²⁺ and ammonium as counterbalancing ions. The synthesis was also carried out using the hydrothermal method, in which the ammonium ions were included in the lattice by adding (NH₄)₂HPO₄ to the reaction mixture [57].

All the abovementioned compounds were described as having the same degree of protonation of the $[V_{12}B_{18}O_{60}]$ core, thus being based on the $[V_{12}B_{18}O_{60}H_6]^{10-}$ polyanion. The five studied clusters have the same mixed valence ratio of V^{IV} to V^V of 10/2.

Lattices (**1**), (**3**), (**4**), and (**5**) present one crystallographic site for the protonated diamine, while (**2**) presents three crystallographically different sites for the (1,3-diapH₂)²⁺ cations. The (1,3-diapH₂)²⁺ ions in lattices (**2**) and (**5**) adopt a “W”-type conformation [66]. In lattices (**2**) and (**3**), the diammonium cations do not adopt a preferential order in the lattice, whereas the (H₃teta)³⁺ molecules in framework (**4**) are defined by the authors as forming pseudo-hexagonal channels [34]. In framework (**5**), the (1,3-diapH₂)²⁺ cations are described as all oriented along the *c* axis [57]. Within all the crystalline

lattices, each protonated diamine connects four $[V_{12}B_{18}O_{60}H_6]^{10-}$ clusters through unidirectional, bifurcated, and trifurcated hydrogen bonds, thus generating supramolecular structures [59].

Table 1. List of the lattices with protonated amines as counterbalancing ions. The mixed valence V^{IV}/V^V ratio is indicated for each lattice.

Compound	Formula	V^{IV}/V^V Ratio	Ref.
1	$(enH_2)_5\{(VO)_{12}O_6[B_3O_6(OH)]_6\} \cdot H_2O$	10/2	[42]
2	$(1,3\text{-diapH}_2)_5\{(VO)_{12}O_6[B_3O_6(OH)]_6\} \cdot 6H_2O$	10/2	[42]
3	$(H_2dap)_2H_6\{(VO)_{12}O_6[B_3O_6(OH)]_6(H_2O)\} \cdot 13H_2O$	10/2	[49]
4	$[H_3\text{teta}]_3[V_{12}B_{18}O_{54}(OH)_6(H_2O)] \cdot (H_3O) \cdot 5H_2O$	10/2	[34]
5	$(NH_4)_8(1,3\text{-diapH}_2)[V_{12}B_{18}O_{60}H_6] \cdot 5H_2O$	10/2	[57]

5. $[V_{12}B_{18}O_{60}]$ Cores with Transition Metal Ions and Coordination Compounds as Counterbalancing Cations

The lattices that include transition metal ions and coordination compounds, together with the $[V_{12}B_{18}O_{60}]$ core in their crystallographic packing, are listed in Table 2. In some cases the metal cations are found coordinated to the clusters through the oxygen atoms of the polyanions and to water molecules, while in other cases coordination complexes with organic molecules are bonded to the VBO clusters. Thus, this class of systems can be considered as functionalized polyoxovanadoborates.

Compound (**12**) has a pure inorganic framework that contains six-coordinated Cd^{II} ions and crystallizes in the cubic centrosymmetric space group $Pn\bar{3}$. The asymmetric unit consists of a half of one Cd^{II} ion, two vanadium atoms, and three boron atoms. The divalent cations are connected to the polyanions sharing μ_3 -bridge-oxygen atoms from the $[B_{18}O_{42}]^{30-}$ and $[V_6O_{18}]^{n-}$ fragments of the $[V_{12}B_{18}O_{60}]$ clusters, leading to a porous 3D lattice. The coordination sphere of the Cd^{II} ions is completed with oxygen atoms of water molecules. The Cd^{II} -(μ_3 -O)- B_2 distances range from 2.184(3) to 2.552(3) Å. Despite the fact that diethylenetriamine (dien) was added to the reaction mixture, this amine is not present in the crystalline system (**12**).

Very appealing crystalline structures are formed when metal cations do not act as bridges between clusters, but are only bonded to one $[V_{12}B_{18}O_{60}]$ cluster, thus decorating it as coordination complexes. The first system of this kind is compound (**6**), reported by Zhang *et al.* in 1999 [43]. This compound includes five-coordinated $Zn(en)_2^{2+}$ cations, whose coordination sphere is completed by coordination to the VBO polyanion through one oxygen atom from the polyborate fragment, forming a Zn -(μ_3 -O)- B_2 covalent bond (Zn -O; 2.042(2) Å) (Figure 4a). Lin *et al.* [45] reported compound (**8**), which has six-coordinated $Ni(en)_2^{2+}$ complexes. These complete their coordination sphere with one VBO cluster bonded through two oxygen atoms, thus forming two Ni -(μ_3 -O)- B_2 bonds (Ni -O; 2.086(4) to 2.224(4) Å) (Figure 4b). Zn (teta) $_2^{2+}$ complexes are part of the crystalline system of (**9**) (Figure 4c) reported by Liu and Zhou [48], while Zn (dien) $_2^{2+}$ and $[Zn(dien)_2(H_2O)]^{2+}$ complexes are introduced in the lattice of compound (**10**) (Figure 4d), reported by Liu *et al.* [49]. The M-O distances of the M-(μ_3 -O)- B_2 bonds have values of 1.979(2) Å for (**9**) and 2.001(4) to 2.436(5) Å for (**10**).

Table 2. List of the lattices with transition metal ions and coordination compounds as counterbalancing ions. The mixed valence V^{IV}/V^V ratio is indicated for each lattice.

Compound	Formula	V^{IV}/V^V Ratio	Ref.
6	$[Zn(en)_2]_6[(VO)_{12}O_6B_{18}O_{39}(OH)_3] \cdot 13H_2O$	9/3	[43]
7	$H_3\{[Cu(en)_2]_5[(VO)_{12}O_6B_{18}O_{42}]\} [B(OH)_3]_2 \cdot 16H_2O$	7/5 †	[44]
8	$[Ni(en)_2]_6H_2[(VO)_{12}O_6B_{18}O_{42}] \cdot 15H_2O$	8/4	[45]
9	$[Zn(teta)]_6[(VO)_{12}O_6B_{18}O_{36}(OH)_6](H_2O) \cdot 8H_2O$	12/0	[48]
10	$\{[Zn(dien)]_2[Zn(dien)(H_2O)]_4[(VO)_{12}O_6[B_3O_6(OH)]_6(H_2O)]_2\} \cdot 15H_2O$	12/0	[49]
11	$\{[Cu(dien)(H_2O)]_3V_{12}B_{18}O_{54}(OH)_6(H_2O)\} \cdot 4H_3O \cdot 5.5H_2O$	10/2	[55]
12	$\{[Cd(H_2O)_2]_3V_{12}B_{18}O_{54}(OH)_6(H_2O)\} \cdot 4H_3O \cdot 9.5H_2O$	10/2	[55]
13	$[Zn(H_2teta)_2V_{12}B_{18}O_{54}(OH)_6] \cdot 4H_3O$	10/2	[63]

† Calculated by us according to the stoichiometric formula given by the authors.

Six $M(en)_2^{2+}$ moieties ($M = Zn, Ni$) are coordinated to each VBO polyanion in (6) and (8), while six $Zn(teta)^{2+}$ units are bonded in (9). In (10) there are two $Zn(dien)^{2+}$ and four $[Zn(dien)(H_2O)]^{2+}$ entities coordinated to the same $[V_{12}B_{18}O_{60}]$ core (Figure 4). The fact that (10) presents six different crystallographic positions for the zinc complexes is concordant with its low symmetry, the triclinic crystalline system ($P-1$). Crystalline system (6) is rhombohedral, whereas (8) and (9) both crystallize in a trigonal system presenting one crystallographic site for the metal-amine entities.

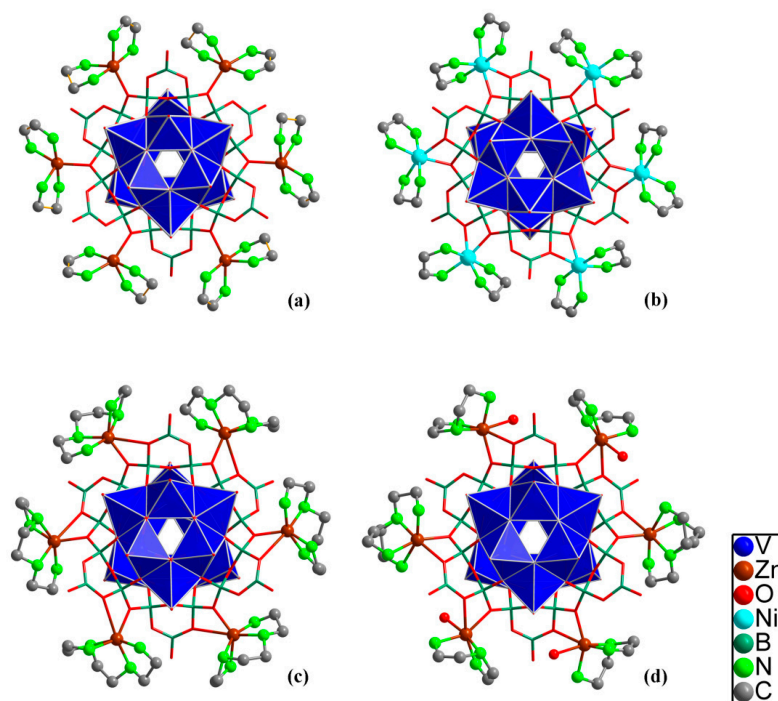


Figure 4. The $[V_{12}B_{18}O_{60}]$ core with the complexes: (a) $Zn(en)_2^{2+}$ for (6), (b) $Ni(en)_2^{2+}$ for (8), (c) $Zn(teta)^{2+}$ for (9), and (d) $Zn(dien)^{2+}$ and $[Zn(dien)(H_2O)]^{2+}$ for (10).

Complexes $Cu(en)_2^{2+}$, $[Cu(dien)(H_2O)]^{2+}$, and $Zn(H_2teta)_2^{2+}$ are part of the crystalline lattices of (7), (11), and (13), respectively, each of them coordinated to the $[V_{12}B_{18}O_{60}]$ clusters. However, in these lattices the

metal-complexes are linking adjacent polyoxovanadoborate cores through V-(μ_2 -O)-M^{II}-(μ_2 -O)-V bonds. In (7) and (11) four and six [V₁₂B₁₈O₆₀] polyanions, respectively, are connected through this type of bonds, while in (13) only two adjacent clusters are linked by the above-mentioned type of bond. The M-O distances range from 2.464(4) to 2.536(4) Å in (7), and 2.033(8) to 2.166(7) Å in (13), while for (11) all distances are 2.292(5) Å.

6. [V₁₂B₁₈O₆₀] Cores with Alkaline Ions as Counterbalancing Cations

Lattices that contain exclusively alkaline cations coordinated to the [V₁₂B₁₈O₆₀] multi-dentate ligands are scarce, in comparison with the lattices that include transition metal ions and organic ammonium ions. To the best of our knowledge, five of the eight reported inorganic frameworks included in this classification, and listed in Table 3, have been published by our research group. Brown *et al.* reported in 2011 the first framework that includes only Na⁺ acting as charge-compensating ions and coordinated to the [V₁₂B₁₈O₆₀] core (14) [51], while one year later Zhou *et al.* published the same compound (14), as (15) [54]. The crystalline lattices (18), (19), (20), and (21) were obtained using the same hydrothermal synthesis conditions as for (14). In comparison with the aforementioned systems, compounds (15), (16), and (17) were obtained by adding auxiliary reducing agents to the reaction mixtures (Na₂SO₃, K₂SO₃, Ni, Co). Despite this fact, all the studied crystalline lattices included in this section present the same 10V^{IV}/2V^V mixed valence ratio. Sodium ions from the isostructural crystalline lattices (14) and (15) are coordinated to six oxygen atoms in a distorted octahedral coordination environment, with Na-O bond lengths ranging from 2.218(5) to 3.040(4) Å for (14) and 2.265(3) to 2.843(1) Å for (15). Zhou *et al.* mentioned that the alternating -Na-O-Na- connectivities in (15) generate 14-ring channels in the (100) direction, where the [V₁₂B₁₈O₆₀] clusters are found, thus permitting a 3D growth of the inorganic framework [54]. Lattices (16) to (19) contain only potassium cations coordinated to oxygen atoms from the VBO polyanionic ligands and/or from water molecules. These ions are found in the form of [K_{O_x]⁺ units in different crystallographic sites and with different coordination geometries. [K_{O_x]⁺ units with $x = 6, 7, 8, 9,$ and 10 are found in (16) and (17), with K-O distances ranging from 2.610(2) to 3.420(6) Å. In compounds (18) and (19), as reported by Hermosilla-Ibáñez *et al.* [57], the K⁺ ions are coordinated to six and seven oxygen atoms, with K-O bonds ranging from 2.468(3) to 3.060(2) Å and 2.625(5) to 3.064(3) Å, respectively. (20) has two different alkaline ions (K⁺ and Cs⁺) in its crystalline lattice. The potassium cations are found to be six- and seven-coordinated (K-O; 2.662(5) to 3.408(4) Å), while cesium cations are always eight-coordinated (Cs-O; 2.970(3) to 3.516(4) Å).}}

Hermosilla-Ibáñez *et al.* reported in 2014 the first framework of the VBO family (21) that contains the alkaline ions with the smallest ionic radius (Li⁺). To the best of our knowledge, this is the sole example of a lattice with lithium counterions [58]. This compound crystallizes in the centrosymmetric cubic space group *Pn-3*, being the first example of such high symmetry. The literature reports examples of crystalline systems with lower symmetries [51,57,67]. Two of the three different crystallographic types of lithium cations are five-coordinated, and one is six-coordinated. The Li-O distances for the five-coordinated ions range from 1.921(2) to 2.976(4) Å, and have values of 3.142(3) Å for the six-coordinated Li⁺ centers. Due to the long Li-O distances of the six-coordinated centers, the authors classified the observed distances as pseudo-coordinative interactions [58].

Table 3. List of the lattices with alkaline ions as counterbalancing cations. The mixed valence V^{IV}/V^V ratio is indicated for each lattice.

Compound	Formula	V^{IV}/V^V Ratio	Ref.
14	(Na) ₁₀ [(H ₂ O)V ₁₂ B ₁₈ O ₆₀ H ₆] 18H ₂ O	10/2	[51]
15	{Na ₂ B ₁₈ V ₁₂ O ₅₄ (OH) ₆ (H ₂ O)[Na ₈ (H ₂ O) ₁₆]} 2H ₂ O	10/2	[54]
16	{K ₂ V ₁₂ B ₁₈ O ₅₄ (OH) ₆ (H ₂ O)[K ₈ (H ₂ O) ₁₆]} 3H ₂ O	10/2	[67]
17	{K ₁₀ V ₁₂ B ₁₈ O ₅₄ (OH) ₆ (H ₂ O)} 14H ₂ O	10/2	[67]
18	K ₈ (NH ₄) ₂ [V ₁₂ B ₁₈ O ₆₀ H ₆] 18H ₂ O	10/2	[57]
19	K ₁₀ [V ₁₂ B ₁₈ O ₆₀ H ₆] 10H ₂ O	10/2	[57]
20	K ₈ CS ₂ [V ₁₂ B ₁₈ O ₆₀ H ₆] 10H ₂ O	10/2	[57]
21	Li ₈ (NH ₄) ₂ [V ₁₂ B ₁₈ O ₆₀ H ₆] 8.02H ₂ O	10/2	[58]

7. [V₁₂B₁₈O₆₀] Cores with Organic Ammonium, Alkaline, and/or Transition Metal Ions as Counterbalancing Cations: The Mixed Family

Table 4. List of the lattices with organic ammonium, alkaline, and/or transition metal ions as counterbalancing cations. The mixed valence V^{IV}/V^V ratio is indicated for each lattice.

Compound	Formula	V^{IV}/V^V Ratio	Ref.
22	(enH ₂) ₄ Na ₄ H ₃ [(V ₁₂ O ₆ B ₁₈ O ₄₂] 8H ₂ O	9/3	[46]
23	K ₃ Na ₅ (H ₂ NCH ₂ CH ₂ NH ₃) ₂ {(VO) ₁₂ O ₆ [B ₃ O ₆ (OH)] ₆ }(H ₂ O) 12H ₂ O	10/2	[47]
24	Na ₈ [Cu(en) ₂] ₂ [V ₁₂ B ₁₈ O ₆₀ H ₆](NO ₃) ₂ 14.7H ₂ O	8/4	[51]
25	Na ₇ [Cu(en) ₂] ₂ [V ₁₂ B ₁₈ O ₆₀ H ₆](NO ₃) 15.5H ₂ O	8/4	[51]
26	[Na(H ₂ O)] ₂ [Na(H ₂ O)] ₂ [Cu(en) ₂][V ₁₂ B ₁₈ O ₅₄ (OH) ₆](H ₃ O) ₂ (H ₂ O) ₁₈	8/4	[50]
27	{[Na(H ₂ O)] ₄] ₃ [V ₁₂ B ₁₈ O ₅₄ (OH) ₆ (H ₂ O)] ₂ }(H ₄ tren) ₄ (H ₃ O) 41H ₂ O	10/2	[53]
28	Na ₈ (H ₃ O){[Ni(H ₂ O)] ₅ [V ₁₂ B ₁₈ O ₆₀ H ₆]} 12.5H ₂ O	11/1	[52]
29	Na ₅ (H ₃ O) ₄ {[Ni(H ₂ O)] ₃ (en)[V ₁₂ B ₁₈ O ₆₀ H ₆]} 9H ₂ O	11/1	[52]
30	Na ₉ (H ₃ O){Zn _{0.5} [V ₁₂ B ₁₈ O ₆₀ H ₆]} 11H ₂ O	11/1	[52]
31	[Hen][H ₂ en]{[Zn(en)] ₂] ₃ [V ₁₂ B ₁₈ O ₆₀ H ₆]} 3H ₂ O	9/3	[52]
32	{[Na(H ₂ O)] ₃] ₄ Na ₂ V ₁₂ B ₁₈ O ₅₆ (OH) ₄ (H ₂ O)}(H ₃ dien) ₂	10/2	[55]
33	{V ₁₂ B ₁₈ O ₅₄ (OH) ₆ (H ₂ O)[K ₆ (H ₂ O) ₁₂]} 2(H ₂ dien) 3H ₂ O	10/2	[67]
34	K ₆ (CH ₃ NH ₃) ₄ [V ₁₂ B ₁₈ O ₅₄ (OH) ₆ (H ₂ O)] 2en 12H ₂ O	10/2	[68]
35	K(H ₃ O)(enH ₂) ₄ [V ₁₂ B ₁₈ O ₆₀ H ₆] 9.60H ₂ O	10/2	[58]
36	K ₅ (H ₃ O) ₂ (1,3-diapH ₂) ₂ [V ₁₂ B ₁₈ O ₆₀ H ₆] 10.8H ₂ O	11/1	[59]
37	K ₂ (H ₃ O) ₇ (enH ₂)[V ₁₂ B ₁₈ O ₆₀ H ₆] 9.0H ₂ O	11/1	[59]
38	[Zn(H ₃ tepa)V ₁₂ B ₁₈ O ₅₄ (OH) ₆][H ₂ en] ₂ H ₃ O 3H ₂ O	10/2	[63]
39	[V ₁₂ B ₁₈ Zn ₃ O ₆₃ H ₁₂] 3(C ₄ N ₃ H ₁₆) 10NH ₄ 5H ₂ O	-	[56]
40	[V ₁₂ B ₁₈ Mn ₃ O ₆₃ H ₁₂] 3(C ₄ N ₃ H ₁₆) 10NH ₄ 5H ₂ O	-	[56]
41	[V ₁₂ B ₁₈ Ni ₃ O ₆₃ H ₁₂] 3(C ₄ N ₃ H ₁₆) 10NH ₄ 5H ₂ O	-	[56]

The systems that include organic ammonium ions along with alkaline and/or transition metal ions in their frameworks are listed in Table 4. (22), (23), (27), (32), (33), (34), (35), (36), and (37) contain alkaline ions and protonated amine ions with different degrees of protonation. Sodium cations are present in the crystalline lattices of (22), (27), and (32) together with protonated ethylenediamine (en),

tris(2-aminoethyl)amine (tren), and diethylenetriamine (dien) molecules, respectively. Lin *et al.* classified framework (22) as a two-dimensional lattice built of Na^+ coordinated to the VBO clusters [46], while (27) is described by Zhou *et al.* as a 1D crystalline system considering the Na-POM connectivities [53]. The coordination of Na^+ to oxygen atoms of the polyanionic clusters, together with the hydrogen bond interactions between the protonated amines and the POM, stabilize the three-dimensional lattice (32). Additionally to the Na^+ , (23) includes K^+ in its 3D crystalline lattice along with monoprotonated ethylenediamine (Hen). In this compound, sodium ions are seven-coordinated (Na-O: 2.335 to 3.500 Å), whereas potassium cations are nine-coordinated (K-O: 2.640 to 3.302 Å). Systems (33), (34), (35), (36), and (37) contain K^+ along with protonated amine ions in their frameworks. Diprotonated dien is found in (33) while diprotonated en is present in (35) and (37); lattice (36) contains 1,3-propanediammonium cations. Methylammonium cations are present in framework (34) due to the decomposition of the ethylenediamine added to the reaction mixture [68]. Potassium cations are coordinated to different oxygen atoms of the vanadyl groups and borate fragments (terminal and bridging groups), and from water molecules, being six-, seven-, eight-, and nine-coordinated, with K-O distances ranging from 2.507(2) to 3.430(7) Å in (33), 2.729(3) to 3.326(3) Å in (34), 2.774(5) to 2.865(5) Å for (35), 2.552(6) to 3.108(6) Å for (36), and 2.140(2) to 3.090(7) Å for (37). The crystalline lattice of the abovementioned systems ((33)–(37)) is stabilized by the coordination of the potassium cations to the polyoxometalate anions, and by the different modes of hydrogen bonds (unidirectional, bifurcated, and trifurcated) between the protonated amine molecules and the VBO clusters. In the crystalline packing of (35), (36), and (37), additional auxiliary cations of hydronium ions also stabilize the lattices. The bond valence sum calculation indicated that the VBO clusters in (33), (34), and (35) have a mixed valence ratio of $10\text{V}^{\text{IV}}/2\text{V}^{\text{V}}$, while in (36) and (37) the ratio is $11\text{V}^{\text{IV}}/1\text{V}^{\text{V}}$.

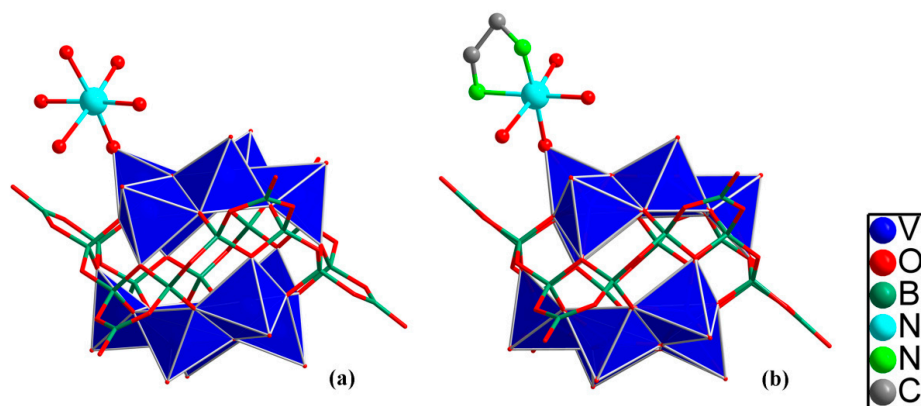


Figure 5. The $[\text{V}_{12}\text{B}_{18}\text{O}_{60}]$ core bonded to: (a) $\text{Ni}(\text{H}_2\text{O})_5^{2+}$ in (28) and (b) $[\text{Ni}(\text{H}_2\text{O})_3(\text{en})]^{2+}$ in (29).

Unlike the crystalline systems previously mentioned within this section that contain protonated amine and alkaline cations, (28), (29), (30), (31), and (38) include coordination complexes of a secondary transition metal ion. Hermosilla-Ibáñez *et al.* in 2012 reported four new compounds based on the $[\text{V}_{12}\text{B}_{18}\text{O}_{60}]$ core, whose negative charge is stabilized by $\text{Ni}(\text{H}_2\text{O})_5^{2+}$, Na^+ and H_3O^+ in (28), by $[\text{Ni}(\text{H}_2\text{O})_3(\text{en})]^{2+}$, Na^+ and H_3O^+ in (29), by Zn^{II} , Na^+ and H_3O^+ in (30), and by $\text{Zn}(\text{en})_2^{2+}$, Hen^+ and

H_2en^{2+} in (31) [52]. Each of the $\text{Ni}(\text{H}_2\text{O})_5^{2+}$ and $[\text{Ni}(\text{H}_2\text{O})_3(\text{en})]^{2+}$ complexes in (28) and (29), respectively, are coordinated to the $[\text{V}_{12}\text{B}_{18}\text{O}_{60}]$ cluster through only one oxygen atom from a vanadyl group (Figure 5). This connection type differs from system (8) described above and reported by Lin *et al.* [45], in which six $\text{Ni}(\text{en})_2^{2+}$ complexes are connected to two oxygen atoms from the borate fragment ($\text{Ni}-(\mu_3\text{-O})\text{-B}_2$) of the VBO polyanion (Figure 4b). Each zinc cation with partial occupancy (0.5) in (30) is four-coordinated to two vanadyl oxygen atoms and to two B-O-B oxygen bridges from two adjacent polyoxovanadoborates (Zn-O distances of 2.337(7) and 2.457(7) Å). Lattices (31) and (38) contain six-coordinated zinc complexes bonded to the $[\text{V}_{12}\text{B}_{18}\text{O}_{60}]$ clusters. Two en molecules and two oxygen-bridging atoms (B-O-B) from the same polyanion are bonded to the Zn^{II} in (31), while two tetraethylenepentamine (tepa) molecules, in addition to two vanadyl oxygen atoms from adjacent polyanions, are coordinated to the Zn^{II} in (38). The electroneutrality of both compounds is attained by protonated ethylenediamine ions, which allow the stabilization of the crystalline frameworks by hydrogen bonds. Additionally, (31) can be compared with compound (6) due to the fact that the latter contains six $\text{Zn}(\text{en})_2^{2+}$ complexes connected to one $[\text{V}_{12}\text{B}_{18}\text{O}_{60}]$ core, while (31) contains only three $\text{Zn}(\text{en})_2^{2+}$ complexes coordinated to the same polyoxometalate.

8. Coordination Geometry Analysis of the Counterbalancing Alkaline and Secondary Transition Metal Ions

On the basis of the crystallographic data included in the literature, we have calculated the best geometry for the alkaline and transition metal ions included in the corresponding crystalline lattices based on the $[\text{V}_{12}\text{B}_{18}\text{O}_{60}]$ core, using the SHAPE 2.1 program [69]. To carry out this study, the maximum M–O distance used to defined the coordination sphere for $\text{M} = \text{Na}^+$ and K^+ is 3.1 Å. In (16) Zhou *et al.* considered a longer K–O coordination distance of 3.4 Å, thus defining a 10-coordinate mode for some of the potassium ions, which is not included in our analysis [67].

Among all the counterbalancing alkaline ions of the $[\text{V}_{12}\text{B}_{18}\text{O}_{60}]$ polyanions, Li^+ is found to be five-coordinated, with a square pyramidal geometry (SPY-5) [58], while Cs^+ is eight-coordinated in a hexagonal bipyramidal geometry (HBPY-8) [57]. On the other hand, Na^+ and K^+ are found with more than one coordination number. As we reported earlier for (14), hexa-coordinated Na^+ ions are found with octahedral (OC-6) and trigonal prismatic (TPR-6) geometries [58]. Nevertheless, extra geometries for the $[\text{NaO}_x]$ are determined by the different coordination numbers ($x = 5$ and 6) in the other systems based on the $[\text{V}_{12}\text{B}_{18}\text{O}_{60}]$ cluster that contain sodium ions in their crystalline packing. As expected, potassium ions with a bigger ionic radius than sodium ions present coordination numbers from six to nine, as has been previously found in the literature [70–72]. Three different geometries are found when K^+ are six-coordinated, two when seven-coordinated, two when eight-coordinated, and one when nine-coordinated. The corresponding geometries are listed in Table 5.

In the case of Mn^{II} , Ni^{II} , Cu^{II} , and Zn^{II} , four- and six-coordination is found, as can be seen in Table 5. Only the six-coordinated manganese ions, which occupy only one crystallographic site in framework (40), adopt the trigonal prismatic geometry (TPR-6). The six-coordinated Ni^{II} ((8), (28), (29) and (41)), Cu^{II} ((7), (11), (24), (25), and (26)) and Zn^{II} ((9), (10), (13), (31), and (38)) share an octahedral geometry (OC-6). The square planar geometry mode (SP-4) is only found for Cu^{II} included in lattices (24) and (25). Zn^{II} presents the highest plasticity among the other transition metal ions, with coordination

numbers four, five, and six. The four-coordinated Zn^{II} ions are in a tetrahedral geometry (T-4), whereas the five-coordinated Zn^{II} ions are found to be in a square pyramidal geometry (SPY-5) and vacant octahedral (vOC-5) geometries.

Table 5. List of the best geometries estimated for the alkaline and transition metal ions, using SHAPE 2.1.

Cation	Geometry	Geometry Symbol
Li	Square Pyramid	(SPY-5)
	Vacant Octahedron	(vOC-5)
Na	Trigonal Bipyramid	(TBPY-5)
	Square Pyramid	(SPY-5)
	Pentagonal Pyramid	(PPY-6)
	Octahedron	(OC-6)
	Trigonal Prism	(TPR-6)
	Pentagonal Pyramid	(PPY-6)
K	Octahedron	(OC-6)
	Trigonal Prism	(TPR-6)
	Capped Octahedron	(COC-7)
	Capped Trigonal Prism	(CTPR-7)
	Square Antiprism	(SAPR-8)
	Triangular Dodecahedron	(TDD-8)
	Tricapped Trigonal Prism	(TCTPR-9)
Cs	Hexagonal Bipyramid	(HBPY-8)
Mn	Trigonal Prism	(TPR-6)
Ni	Octahedron	(OC-6)
Cu	Square	(SP-4)
	Octahedron	(OC-6)
Zn	Tetrahedron	(T-4)
	Square Pyramid	(SPY-5)
	Vacant Octahedron	(vOC-5)
	Octahedron	(OC-6)

9. Spectroscopic Properties

The FT-IR fingerprint region characteristic of the [V₁₂B₁₈O₆₀] core is observed between *ca.* 640 and 1420 cm⁻¹. The asymmetric and symmetric V–O–V stretching vibrations appear in the low energy region between 640 and 880 cm⁻¹, whereas the bands observed in the range of 900 and 960 cm⁻¹ are assigned to the terminal V–O stretching vibrations of the vanadyl group. On the other hand, the borate fragments are characterized by B–O asymmetrical stretching vibrations for both the [BO₃] and [BO₄] units, appearing between 1020 and 1150 cm⁻¹ for the trigonal and between 1300 and 1420 cm⁻¹ for the tetrahedral units [34,43,44,48–50,52–55,57,58,63,67,68]. Müller *et al.* reported that the energy and shape of the vanadyl stretching bands depend on the oxidation state and on the existing interactions of the vanadyl groups of the polyoxovanadate anions in the crystalline packing [26]. In the IR spectra reported for all the studied systems, only (11) presents a sharp stretching vibration of the terminal V–O

group. This fact can be rationalized considering that in this framework the polyanion has all the vanadyl groups equally connected to $[\text{Cu}(\text{dien})(\text{H}_2\text{O})]^{2+}$ complexes.

The optical properties of compounds (4), (5), (7), (9), (10), (12), (15), (16), (18), (19), (20), (21), (27), (29), (30), (35), and (38) have been studied by solid-state diffuse reflectance spectroscopy in the UV-visible region, since they are all insoluble in most common organic solvents and water. Three bands in the studied UV-visible region are reported for almost all the investigated systems: two bands in the high energy region, between 243 and 230 nm, and 344 and 310 nm, depending on the species, and one band that appears between 590 to 517 nm. In general, the two absorption bands in the high energy region are assigned as $\text{O} \rightarrow \text{V}$ and $\text{O} \rightarrow \text{B}$ charge transfer transitions, respectively. The less intense band in the low energy region has been assigned to Intervalence Charge Transfer Transitions (IVCT) and to d–d transitions [34,48,52–55,57,58,63,67]. With respect to the low energy absorption bands (*ca.* 500 nm), most authors consider that these arise from “presumably d-d electronic transitions” [34,53,54,63]. With respect to the bands in this same visible region of the polymetallic vanadium species, Robin and Day consider that they should be assigned to mixed valence absorptions [73]. However, the real meaning of these bands should become apparent once a more complete electronic description has been attained from quantum mechanical calculations. We are currently calculating the electronic spectra of these species by DFT methods.

Considering the similarity of the UV-visible spectra of these systems even when the polyanions are functionalized with secondary transition metal atoms [52], we can deduce that the crystalline lattices have a negligible effect on the electronic properties of the $[\text{V}_{12}\text{B}_{18}\text{O}_{60}]$ core.

10. Magnetic Properties

Among all the studied compounds included in this review, the magnetic properties of only (5), (11), (12), (15), (18), (19), (27), and (38) have been reported [53–55,57,63]. All of these systems have a mixed valence ratio of $10\text{V}^{\text{IV}}/2\text{V}^{\text{V}}$, and present a bulk antiferromagnetic behavior. The χT values at 300 and 2 K for the abovementioned compounds are listed in Table 6. (11) presents the highest χT value of 4.81 emu K mol^{-1} , which was explained by Zhou *et al.*, assuming that this value is very close to the theoretical χT value of 4.88 emu K mol^{-1} , considering 10 uncoupled V^{IV} plus three uncoupled Cu^{II} centers ($g = 2.00$ for both atoms) [55]. However, when the χT value of the three uncoupled Cu^{II} centers is subtracted ($g = 2.00$), the resultant χT value for the $[\text{V}_{12}\text{B}_{18}\text{O}_{60}]$ polyanion of (11) is 3.68 emu K mol^{-1} , thus presenting the same trend followed by (5), (12), (15), (18), (19), and (27) (Figure 6). From the $\chi T(T)$ graph reported by Zhou *et al.* [53] it is possible to infer that (27) is almost magnetically uncoupled at room temperature. On the other hand, the χT values of the rest of compounds, (5), (12), (15), (18), and (19) show that all of them are magnetically coupled at room temperature. Within the observed tendency of 3.34 to 3.83 emu K mol^{-1} , there is no clear correlation between the magnetic properties and the nature of the frameworks, which include different cations interacting with the polyanions, even though it is clear that the interactions between the different cations and the polyanion in the lattice affect the magnitude of the exchange phenomena in the cluster.

It is interesting to point out that Hermosilla-Ibáñez *et al.* reported in 2014 that it is possible to show by DFT calculations that the alkaline ions in compounds (18) and (19) quench the intracuster antiferromagnetic coupling, in comparison with compound (5) [57]. In this study, the results indicated

that the presence of alkaline ions perturbs the extent of the spin density of the magnetic orbitals (d_{xy}); this perturbation is dependent on the distance between the alkaline cation and the oxygen of the vanadyl groups. Thus, the obtained modification of the orbital overlap due to the presence of the alkaline cations influences the magnitude of the antiferromagnetic interactions. Nevertheless, the existence of additional hydrogen bonds and/or covalent bonds should also influence the global magnetic properties.

As can be seen, the most coupled system is (38), which includes $\text{Zn}(\text{H}_3\text{tepa})^{2+}$ and $(\text{enH}_2)^{2+}$ as counterbalancing ions. In this system the $\text{Zn}(\text{H}_3\text{tepa})^{2+}$ complexes are coordinated to the $[\text{V}_{12}\text{B}_{18}\text{O}_{60}]$ polyanions through two oxygen atoms of vanadyl groups from adjacent polyoxovanadoborates, *i.e.*, acting as bridges between two polyanions. As discussed above, the coordination of the vanadyl groups with a cation influences the electronic properties, *i.e.* stretching vibrations and exchange interactions. In (38) the presence of the zinc(II) cations bridging the polyanion clearly increases the antiferromagnetic behavior of the material.

Table 6. List of the reported compounds with magnetic property studies.

Compound	Auxiliary cations	$\text{V}^{\text{IV}}/\text{V}^{\text{V}}$ Ratio	χT (emu K mol ⁻¹) (300 K)	χT (emu K mol ⁻¹) (2 K)	Ref.
5	NH_4^+ , $(1,3\text{-diapH}_2)^{2+}$	10/2	3.34	0.33	[57]
11	$[\text{Cu}(\text{dien})(\text{H}_2\text{O})]^{2+}$	10/2	4.81 (3.68) *	0.56	[55]
12	$\text{Cd}(\text{H}_2\text{O})_2^{2+}$	10/2	3.60	0.10	[55]
15	Na^+	10/2	3.53	0.23	[54]
18	K^+ , NH_4^+	10/2	3.57	0.40	[57]
19	K^+	10/2	3.58	0.38	[57]
27	$[\text{Na}(\text{H}_2\text{O})_4]^+$, $(\text{H}_4\text{tren})^{4+}$	10/2	3.83	0.15	[53]
38	$\text{Zn}(\text{H}_3\text{tepa})^{2+}$, $(\text{enH}_2)^{2+}$	10/2	1.54	0.11	[63]

* The χT value in parentheses is the χT value of the polyanion, which was calculated by subtracting the χT value for the three uncoupled Cu^{II} centers, considering a $g = 2$ ($\chi T = 1.13$ emu K mol⁻¹).

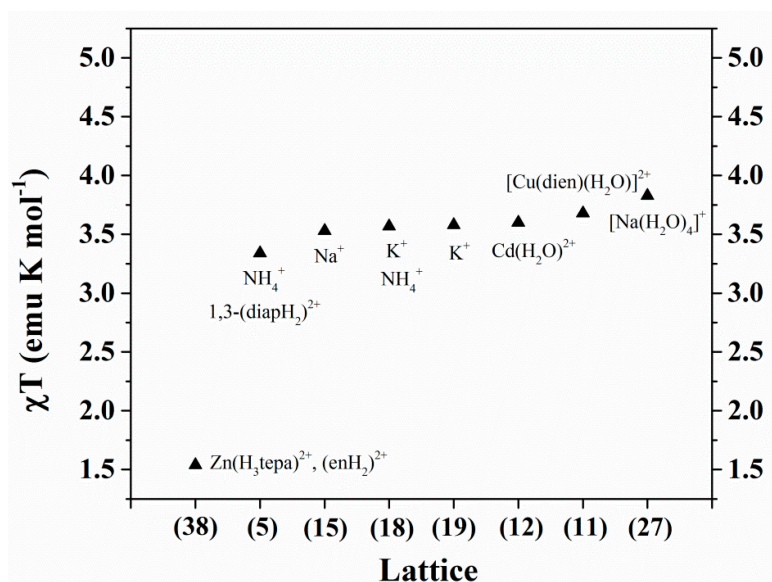


Figure 6. χT values for each lattice.

11. Final Remarks

The structural stability of the $[V_{12}B_{18}O_{60}]$ core allows the formation of polyoxometalate species with different crystalline lattices, depending on the cations present in the synthesis. This polyanion is potentially able to share bridging B-O-B oxygen atoms, both vanadyl and bridging B-O-B oxygen atoms, and in some cases, the 12 oxygen atoms from the vanadyl groups, thus permitting one-, two-, or three-dimensional frameworks to be obtained. The presence of auxiliary cations may be responsible for the alignment of the organic amines in only one direction, since they can fill hindered nucleophilic sites around the polyanions.

Hermosilla-Ibáñez *et al.* demonstrated that the organic diamines act as reducing agents in the reactions, as the presence of nitrate ions in the final mother liquors was detected by ionic liquid chromatography [57]. The FT-IR results show that the coordination of a cation to each of the existing vanadyl groups of the polyanion produces a single and sharp stretching band for the vanadyl group. Thus, the coordination of the vanadyl groups with cations influences the electronic properties, *i.e.*, stretching vibrations and exchange interactions. However, the similarity of the solid state reflectance spectra indicates that the crystalline lattices have a negligible effect on the electronic spectra of the $[V_{12}B_{18}O_{60}]$ core.

From the reported magnetic data it is clear to conclude that the $[V_{12}B_{18}O_{60}H_6]$ cluster with a $10V^{IV}/2V^V$ mixed-valence ratio presents a global antiferromagnetic exchange among the 10 spin carriers. It can also be concluded that the interactions of the cations in the crystal packing with the polyanion can modify the global antiferromagnetic interaction in the polyanion. Further studies must be done in order to reach a deeper understanding of the magnetic behavior in these compounds. At this time our group is working on the rationalization of the magnetic properties of the $[V_{12}B_{18}O_{60}]$ family.

Acknowledgments

The authors acknowledge financial support from projects FONDECYT 1120004 and Financiamiento Basal FB0807 (CEDENNA). This work was done under the international collaborative project LIA-MIF 836. Powered@ NLHPC: This research was partially supported by the super-computing infrastructure of the NLHPC (ECM-02), Centre for Mathematical Modelling CMM, Universidad de Chile. KMB thanks 21100772 and AT-24121391 doctoral scholarships and the USACH-French Embassy agreement for a doctoral mobility grant. PHI thanks Vicerrectoría de Investigación, Desarrollo e Innovación (USACH) for the POSTDOC_DICYT 001316 scholarship.

Author Contributions

The manuscript was written with equal contributions from all authors. DVY owns the general idea and plan of the publication. Most of the presented results are part of the Doctoral thesis of PHI and KMB. ES and VPG were part of the discussion and analysis of the presented data. ELF collaborated with the structural determinations.

Conflicts of Interest

The authors declare no conflict of interest.

References

1. Pope, M.T.; Müller, A. *Polyoxometalate Chemistry From Topology via Self-Assembly to Applications*. Kluwer Academic Publishers: Dordrecht, The Netherlands, 2001.
2. Yamase, T.; Pope, M.T. *Polyoxometalate Chemistry for Nano-Composite Design*; Kluwer Academic: Dordrecht, The Netherlands; Plenum Publishers: New York, NY, USA, 2002.
3. Borrás-Almenar, J.J.; Coronado, E.; Müller, A.; Pope, M.T. *Polyoxometalate Molecular Science*; Kluwer Academic Publishers: Dordrecht, The Netherlands, 2003.
4. Müller, A.; Peters, F.; Pope, M.T.; Gatteschi, D. Polyoxometalates: Very large clusters-nanoscale magnets. *Chem. Rev.* **1998**, *98*, 239–271.
5. Clemente-Juan, J.M.; Coronado, E.; Gaita-Ariño, A. Magnetic polyoxometalates: from molecular magnetism to molecular spintronics and quantum computing. *Chem. Soc. Rev.* **2012**, *41*, 7464–7478.
6. Suzuki, K.; Sato, R.; Mizuno, N. Reversible switching of single-molecule magnet behaviors by transformation of dinuclear dysprosium cores in polyoxometalates. *Chem. Sci.* **2013**, *4*, 596–600.
7. Mizuno, N.; Misono, M. Heterogeneous catalysis. *Chem. Rev.* **1998**, *98*, 199–217.
8. Lv, H.; Geletii, Y.V.; Zhao, C.; Vickers, J.W.; Zhu, G.; Luo, Z.; Song, J.; Lian, T.; Musaev, D.G.; Hill, C.L. Polyoxometalate water oxidation catalysts and the production of green fuel. *Chem. Soc. Rev.* **2012**, *41*, 7572–7589.
9. Rhule, J.T.; Hill, C.L.; Judd, D.A.; Schinazi, R.F. Polyoxometalates in medicine. *Chem. Rev.* **1998**, *98*, 327–357.
10. Wang, Y.; Weinstock, I.A. Polyoxometalate-decorated nanoparticles. *Chem. Soc. Rev.* **2012**, *41*, 7479–7496.
11. Miras, H.N.; Yan, J.; Long, D.-L.; Cronin, L. Engineering polyoxometalates with emergent properties. *Chem. Soc. Rev.* **2012**, *41*, 7403–7430.
12. Song, Y.-F.; Tsunashima, R. Recent advances on polyoxometalate-based molecular and composite materials. *Chem. Soc. Rev.* **2012**, *41*, 7384–7402.
13. Long, D.-L.; Tsunashima, R.; Cronin, L. Polyoxometalates: Building blocks for functional nanoscale systems. *Angew. Chem. Int. Ed.* **2010**, *49*, 1736–1758.
14. Streb, C.; Long, D.-L.; Cronin, L. Influence of organic amines on the self-assembly of hybrid polyoxo-molybdenum(V) phosphate frameworks. *CrystEngComm* **2006**, *8*, 629–634.
15. Yi, Z.; Yu, X.; Xia, W.; Zhao, L.; Yang, C.; Chen, Q.; Wang, X.; Xu, X.; Zhang, X. Influence of the steric hindrance of organic amines on the supramolecular network based on polyoxovanadates. *CrystEngComm.* **2010**, *12*, 242–249.
16. Long, D.-L.; Kögerler, P.; Farrugia, L.J.; Cronin, L. Restraining symmetry in the formation of small polyoxomolybdates: Building blocks of unprecedented topology resulting from “shrink-wrapping” $[H_2Mo_{16}O_{52}]^{10-}$ -type clusters. *Angew. Chem. Int. Ed.* **2003**, *42*, 4180–4183.
17. Abbas, H.; Pickering, A.L.; Long, D.-L.; Kögerler, P.; Cronin, L. Controllable growth of chains and grids from polyoxomolybdate building blocks linked by Silver(I) dimers. *Chem. Eur. J.* **2005**, *11*, 1071–1078.

18. Streb, G.; McGlone, T.; Brücher, O.; Long, D.-L.; Cronin, L. Hybrid host-guest complexes: Directing the supramolecular structure through secondary host-guest interactions. *Chem. Eur. J.* **2008**, *14*, 8861–8868.
19. Mcglone, T.; Streb, C.; Long, D.-L.; Cronin, L. Guest-directed supramolecular architectures of {W₃₆} polyoxometalate crowns. *Chem. Asian J.* **2009**, *4*, 1612–1618.
20. Day, V.W.; Klemperer, W.G.; Yaghi, O.M. A new structure type in polyoxoanion chemistry: synthesis and structure of the V₅O₁₄³⁻ anion. *J. Am. Chem. Soc.* **1989**, *111*, 4518–4519.
21. Evans, H.T. The molecular structure of the isopoly complex ion, decavanadate (V₁₀O₂₈¹⁶⁻). *Inorg. Chem.* **1966**, *5*, 967–977.
22. Day, V.W.; Klemperer, W.G.; Yaghi, O.M. Synthesis and characterization of a soluble oxide inclusion complex, [CH₃CN⊂(V₁₂O₁₂⁴⁻)]. *J. Am. Chem. Soc.* **1989**, *111*, 5959–5962.
23. Hou, D.; Hagen, K.S.; Hill, C.L. Tridecavanadate, [V₁₃O₃₄]³⁻, a new high-potential isopolyvanadate. *J. Am. Chem. Soc.* **1992**, *114*, 5864–5866.
24. Hou, D.; Hagen, K.S.; Hill, C.L. Pentadecavanadate, V₁₅O₄₂⁹⁻, a new highly condensed fully oxidized isopolyvanadate with kinetic stability in water. *J. Chem. Soc. Chem. Commun.* **1993**, *20*, 426–428.
25. Müller, A.; Krickemeyer, E.; Penk, M.; Walberg, H.-J.; Bögge, H. Spherical mixed-valence [V₁₅O₃₆]⁵⁻, an example from an unusual cluster family. *Angew. Chem. Int. Ed. Engl.* **1987**, *26*, 1045–1046.
26. Müller, A.; Sessoli, R.; Krickemeyer, E.; Bögge, H.; Meyer, J.; Gatteschi, D.; Pardi, L.; Westphal, J.; Hovemeier, K.; Rohlfing, R.; Döring, J.; Hellweg, F.; Beugholt, C.; Schmidtman, M. Polyoxovanadates: High-nuclearity spin clusters with interesting host-guest systems and different electron populations. synthesis, spin organization, magnetochemistry, and spectroscopic studies. *Inorg. Chem.* **1997**, *36*, 5239–5250.
27. Suber, L.; Bonamico, M.; Fares, V. Synthesis, magnetism, and X-ray molecular structure of the mixed-valence vanadium(IV/V)-oxygen cluster [VO₄⊂(V₁₈O₄₅)]⁹⁻. *Inorg. Chem.* **1997**, *36*, 2030–2033.
28. Müller, A.; Krickemeyer, E.; Penk, M.; Rohlfing, R.; Armatage, A.; Bögge, H. Template-controlled formation of cluster shells or a type of molecular recognition: Synthesis of [HV₂₂O₅₄(ClO₄)]⁶⁻ and [H₂V₁₈O₄₄(N₃)]⁵⁻. *Angew. Chem. Int. Ed.* **1991**, *30*, 1674–1677.
29. Müller, A.; Rohlfing, R.; Döring, J.; Penk, M. Formation of a cluster sheath around a central cluster by a “self-organization process”: the mixed valence polyoxovanadate[V₃₄O₈₂]¹⁰⁻. *Angew. Chem. Int. Ed.* **1991**, *30*, 588–590.
30. Warren, C.J.; Rijssenbeek, J.T.; Rose, D.J.; Haushalter, R.C.; Zubieta, J. Hydrothermal synthesis and characterization of an unusual polyoxovanadium borate cluster: Structure of Rb₄[(VO)₆{B₁₀O₁₆(OH)₆}]₂ · 0.5H₂O. *Polyhedron* **1998**, *17*, 2599–2605.
31. Williams, I.D.; Wu, M.; Sung, H.H.-Y.; Zhang, X.X.; Yu, J. An organotemplated vanadium(IV) borate polymer from boric acid “flux” synthesis, [H_{2en}]₄[Hen]₂[V₆B₂₂O₅₃H₈] · 5H₂O. *Chem. Commun.* **1998**, 2463–2464.
32. Cao, Y.-N.; Zhang, H.-H.; Huang, C.-C.; Sun, Y.-X.; Chen, Y.-P.; Guo, W.-J.; Zhang, F.-L. Synthesis and structural characterization of a new polyoxovanadium borate: (H₃NCH₂CH₂NH₃)₄[(VO)₆(B₁₀O₂₂)₂](H₃O)₇. *Chin. J. Struct. Chem.* **2005**, *24*, 525–530.

33. Cai, Q.; Lu, B.; Zhang, J.; Shan, Y. Synthesis, structure and properties of $(\text{H}_2\text{NCH}_2\text{CH}_2\text{NH}_3)_3\{(\text{VO})_6[\text{B}_{10}\text{O}_{16}(\text{OH})_6]_2\} \cdot 11\text{H}_2\text{O}$. *J. Chem. Crystallogr.* **2008**, *38*, 321–325.
34. Liu, X.; Zhou, J.; An, L.; Chen, R.; Hu, F.; Tang, Q. Hydrothermal syntheses, crystal structures and characterization of new vanadoborates: The novel decorated cage cluster $[\text{V}_6\text{B}_{22}\text{O}_{44}(\text{OH})_{10}]$. *J. Solid State Chem.* **2013**, *201*, 79–84.
35. Wu, M.; Law, T.S.-C.; Sung, H.H.-Y.; Cai, J.; Williams, I.D. Synthesis of elliptical vanadoborates housing bimetallic centers $[\text{Zn}_4(\text{B}_2\text{O}_4\text{H}_2)(\text{V}_{10}\text{B}_{28}\text{O}_{74})]^{8-}$ and $[\text{Mn}_4(\text{C}_2\text{O}_4)(\text{V}_{10}\text{B}_{28}\text{O}_{74}\text{H}_8)]^{10-}$. *Chem. Commun.* **2005**, *4*, 1827–1829.
36. Cao, Y.; Zhang, H.; Huang, C.; Yang, Q.; Chen, Y.; Sun, R.; Zhang, F.; Guo, W. Synthesis, crystal structure and two-dimensional infrared correlation spectroscopy of a layer-like transition metal (TM)-oxalate templated polyoxovanadium borate. *J. Solid State Chem.* **2005**, *178*, 3563–3570.
37. Chen, H.; Yu, Z.-B.; Bacsik, Z.; Zhao, H.; Yao, Q.; Sun, J. Construction of mesoporous frameworks with vanadoborate clusters. *Angew. Chem. Int. Ed.* **2014**, *53*, 3608–3611.
38. Warren, C.J.; Haushalter, R.C.; Rose, D.J.; Zubieta, J. A bimetallic main group oxide cluster of the oxovanadium borate system: $(\text{H}_3\text{NCH}_2\text{CH}_2\text{NH}_3)_4[(\text{VO})_{12}\text{O}_4\{\text{B}_8\text{O}_{17}(\text{OH})_4\}_2\{\text{Mn}(\text{H}_2\text{O})_2\}_2] \cdot \text{H}_2\text{O}$. *Inorg. Chim. Acta* **1998**, *282*, 123–129.
39. Cao, Y.; Zhang, H.; Huang, C.; Chen, Y.; Sun, R.; Guo, W. Hydrothermal synthesis and crystal structure of a novel 1D polyoxovanadium borate: $(\text{H}_3\text{NCH}_2\text{CH}_2\text{NH}_3)_3[(\text{VO})_{12}\text{O}_4\{\text{B}_8\text{O}_{17}(\text{OH})_4\}_2\{\text{Na}(\text{H}_2\text{O})\}_2(\text{H}_3\text{O})_2(\text{H}_2\text{O})_{6.5}]$. *J. Mol. Struct.* **2005**, *733*, 211–216.
40. Sun, Y.-Q.; Li, G.-M.; Chen, Y.-P. A novel polyoxovanadium borate incorporating an organic amine ligand: synthesis and structure of $[\text{V}_{12}\text{B}_{16}\text{O}_{50}(\text{OH})_7(\text{en})]^{7-}$. *Dalton Trans.* **2012**, *41*, 5774–5777.
41. Liu, X.; Zhou, J.; Xiao, H.-P.; Kong, C.; Zou, H.; Tang, Q.; Li, J. Two new 3-D boratopolyoxovanadate architectures based on the $[\text{V}_{12}\text{B}_{16}\text{O}_{50}(\text{OH})_8]^{12-}$ cluster with different metal linkers. *New J. Chem.* **2013**, *37*, 4077–4082.
42. Rijssenbeek, J.T.; Rose, D.J.; Haushalter, R.C.; Zubieta, J. Novel clusters of transition metals and main group oxides in the alkylamine/oxovanadium/borate system. *Angew. Chem. Int. Ed.* **1997**, *36*, 1008–1010.
43. Zhang, L.; Shi, Z.; Yang, G.; Chen, X.; Feng, S. Hydrothermal synthesis and X-ray single crystal structure of $[\text{Zn}(\text{en})_2]_6[(\text{VO})_{12}\text{O}_6\text{B}_{18}\text{O}_{39}(\text{OH})_3] \cdot 13\text{H}_2\text{O}$. *J. Solid State Chem.* **1999**, *148*, 450–454.
44. Lin, Z.-H.; Zhang, H.-H.; Huang, C.-C.; Sun, R.-Q.; Chen, Y.-P.; Wu, X.-Y. Hydrothermal synthesis, crystal structure and properties of polyoxovanadium borate $\text{H}_3\{[\text{Cu}(\text{en})_2]_5[(\text{VO})_{12}\text{O}_6\text{B}_{18}\text{O}_{42}]\}[\text{B}(\text{OH})_3]_2 \cdot 16\text{H}_2\text{O}$. *Acta Chim. Sin.* **2004**, *62*, 391–398.
45. Lin, Z.-H.; Zhang, H.-H.; Huang, C.-C.; Sun, R.-Q.; Yang, Q.-Y.; Wu, X.-Y. Hydrothermal synthesis and crystal structure of $[\text{Ni}(\text{en})_2]_6\text{H}_2[(\text{VO})_{12}\text{O}_6\text{B}_{18}\text{O}_{42}] \cdot 15\text{H}_2\text{O}$. *Chin. J. Struct. Chem.* **2004**, *23*, 83–86.
46. Lin, Z.-H.; Yang, Q.-Y.; Zhang, H.-H.; Huang, C.-C.; Sun, R.-Q.; Wu, X.-Y. Hydrothermal synthesis and crystal structure of $(\text{enH}_2)_4\text{Na}_4\text{H}_3[(\text{VO})_{12}\text{O}_6\text{B}_{18}\text{O}_{42}] \cdot 8\text{H}_2\text{O}$. *Chin. J. Struct. Chem.* **2004**, *23*, 590–595.
47. Lu, B.; Wang, H.; Zhang, L.; Dai, C.-Y.; Cai, Q.-H.; Shan, Y.-K. Hydrothermal synthesis and structure of $\text{K}_3\text{Na}_5(\text{H}_2\text{NCH}_2\text{CH}_2\text{NH}_3)_2\{(\text{VO})_{12}\text{O}_6[\text{B}_3\text{O}_6(\text{OH})_6]\}(\text{H}_2\text{O}) \cdot 12\text{H}_2\text{O}$. *Chin. J. Chem.* **2005**, *23*, 137–143.

48. Liu, X.; Zhou, J. The new vanadoborate-supported hexanuclear zinc complex $[\text{Zn}(\text{teta})]_6[(\text{VO})_{12}\text{O}_6\text{B}_{18}\text{O}_{36}(\text{OH})_6](\text{H}_2\text{O})_8 \cdot 8\text{H}_2\text{O}$. *Z. Naturforsch.* **2011**, *66b*, 115–118.
49. Liu, X.; Zhou, J.; Zhou, Z.; Zhang, F. Hydrothermal syntheses and crystal structures of two new heteropolyoxovanadoborates containing $\{(\text{VO})_{12}\text{O}_6[\text{B}_3\text{O}_6(\text{OH})_6](\text{H}_2\text{O})\}$ cluster. *J. Clust. Sci.* **2011**, *22*, 65–72.
50. Li, G.-M.; Mei, H.-X.; Chen, X.-Y.; Chen, Y.-P.; Sun, Y.-Q.; Zhang, H.-H.; Chen, X.-P. A porous organic-inorganic hybrid compound constructed from polyoxovanadium borate anions, dinuclear Na sites and metal-organic units. *Chin. J. Struct. Chem.* **2011**, *30*, 785–792.
51. Brown, K.; Car, P.-E.; Vega, A.; Venegas-Yazigi, D.; Paredes-García, V.; Vaz, M.G.F.; Allao, R.A.; Pivan, J.-Y.; Le Fur, E.; Spodine, E. Polyoxometalate cluster $[\text{V}_{12}\text{B}_{18}\text{O}_{60}\text{H}_6]$ functionalized with the copper(II) bis-ethylenediamine complex. *Inorg. Chim. Acta* **2011**, *367*, 21–28.
52. Hermosilla-Ibáñez, P.; Car, P.E.; Vega, A.; Costamagna, J.; Caruso, F.; Pivan, J.-Y.; Le Fur, E.; Spodine, E.; Venegas-Yazigi, D. New structures based on the mixed valence polyoxometalate cluster $[\text{V}_{12}\text{B}_{18}\text{O}_{60}\text{H}_6]^{n-}$. *CrystEngComm* **2012**, *14*, 5604–5612.
53. Zhou, J.; Liu, X.; Hu, F.; Zou, H.; Li, X. A new 1-D extended vanadoborate containing triply bridged metal complex units. *Inorg. Chem. Commun.* **2012**, *25*, 51–54.
54. Zhou, J.; Liu, X.; Hu, F.; Zou, H.; Li, R.; Li, X. One novel 3-D vanadoborate with unusual 3-D Na–O–Na network. *RSC Adv.* **2012**, *2*, 10937–10940.
55. Zhou, J.; Liu, X.; Chen, R.; Xiao, H.-P.; Hu, F.; Zou, H.; Zhou, Y.; Liu, C.; Zhu, L. New 3-D polyoxovanadoborate architectures based on $[\text{V}_{12}\text{B}_{18}\text{O}_{60}]^{16-}$ clusters. *CrystEngComm* **2013**, *15*, 5057–5063.
56. Chen, H.; Deng, Y.; Yu, Z.; Zhao, H.; Yao, Q.; Zou, X.; Bäckvall, J.E.; Sun, J. 3D open-framework vanadoborate as a highly effective heterogeneous pre-catalyst for the oxidation of alkylbenzenes. *Chem. Mater.* **2013**, *25*, 5031–5036.
57. Hermosilla-Ibáñez, P.; Cañon-Mancisidor, W.; Costamagna, J.; Vega, A.; Paredes-García, V.; Garland, M.T.; Le Fur, E.; Cador, O.; Spodine, E.; Venegas-Yazigi, D. Crystal lattice effect on the quenching of the intracluster magnetic interaction in $[\text{V}_{12}\text{B}_{18}\text{O}_{60}\text{H}_6]^{10-}$ polyoxometalate. *Dalton Trans.* **2014**, *43*, 14132–14141.
58. Hermosilla-Ibáñez, P.; Costamagna, J.; Vega, A.; Paredes-García, V.; Le Fur, E.; Spodine, E.; Venegas-Yazigi, D. Coordination interactions in the crystalline lattice of alkaline ions with the polyoxometalate $[\text{V}_{12}\text{B}_{18}\text{O}_{60}\text{H}_6]^{10-}$ ligand. *J. Coord. Chem.* **2014**, *67*, 3940–3952.
59. Hermosilla-Ibáñez, P.; Costamagna, J.; Vega, A.; Paredes-García, V.; Garland, M.T.; Le Fur, E.; Spodine, E.; Venegas-Yazigi, D. Protonated diamines as linkers in the supramolecular assemblies based on the $[\text{V}_{12}\text{B}_{18}\text{O}_{60}\text{H}_6]$ polyoxovanadoborate anion. *J. Struct. Chem.* **2014**, *55*, 1453–1465.
60. Yamase, T.; Suzuki, M.; Ohtaka, K. Structures of photochemically prepared mixed-valence polyoxovanadate clusters: oblong $[\text{V}_{18}\text{O}_{44}(\text{N}_3)]^{14-}$, superkeggin $[\text{V}_{18}\text{O}_{42}(\text{PO}_4)]^{11-}$ and doughnut-shaped $[\text{V}_{12}\text{B}_{32}\text{O}_{84}\text{Na}_4]^{15-}$ anions. *Dalton Trans.* **1997**, *44*, 2463–2472.
61. Warren, C.J.; Rose, D.J.; Haushalter, R.C.; Zubieta, J. A new transition metal–main group oxide cluster in the oxovanadium–borate system: hydrothermal synthesis and structure of $(\text{H}_3\text{O})_{12}[(\text{VO})_{12}\{\text{B}_{16}\text{O}_{32}(\text{OH})_4\}_2] \cdot 28\text{H}_2\text{O}$. *Inorg. Chem.* **1998**, *37*, 1140–1141.

62. Williams, I.D.; Wu, M.; Sung, H.H.-Y.; Law, T.S.-C.; Zhang, X.X. *Contemporary Boron Chemistry: Synthesis and Properties of Vanadoborate Cluster Materials*; Davidson, M.G., Hughes, A.K., Marder, T.B., Wade, K., Eds.; Royal Society of Chemistry: Cambridge, UK, **2000**.
63. Liu, X.; Zhao, R.; Zhou, J.; Liu, M. Three new vanadoborates functionalized with zinc complexes. *Inorg. Chem. Commun.* **2014**, *43*, 101–104.
64. Christ, C.L.; Clark, J.R. A crystal-chemical classification of borate structures with emphasis on hydrated borates. *Phys. Chem. Miner.* **1977**, *2*, 59–87.
65. Hagrman, P.J.; Finn, R.C.; Zubieta, J. Molecular manipulation of solid state structure: Influences of organic components on vanadium oxide architectures. *Solid State Sci.* **2001**, *3*, 745–774.
66. Zhang, Y.-N.; Zhou, B.-B.; Sha, J.-Q.; Su, Z.-H.; Cui, J.-W. Assembly of two layered cobalt–molybdenum phosphates: Changing interlayer distances by tuning the lengths of amine ligands. *J. Solid State Chem.* **2011**, *184*, 419–426.
67. An, L.; Zhou, J.; Xiao, H.-P.; Liu, X.; Zou, H.; Pan, C.-Y.; Liu, M.; Li, J. A series of new 3-D boratopolyoxovanadates containing five types of $[K_xO_y]_n$ building units. *CrystEngComm* **2014**, *16*, 4236–4244.
68. Meng, Q.; He, H.; Yang, B.-F.; Zhao, J.-W.; Yang, G.-Y. Synthesis and characterization of a 3-D framework constructed from $[V_{12}B_{18}O_{54}(OH)_6(H_2O)]^{10-}$ clusters and K^+ cations. *J. Clust. Sci.* **2014**, *25*, 1273–1282.
69. Llunell, M.; Casanova, D.; Cirera, J.; Alemany, P.; Alvarez, S. *SHAPE*, version 2.1; Universitat de Barcelona, Barcelona, Spain, 2013.
70. Delgado, F.S.; Ruiz-Pérez, C.; Sanchiz, J.; Lloret, F.; Julve, M. Versatile supramolecular self-assembly. Part I. Network formation and magnetic behaviour of the alkaline salts of the bis(malonate)cuprate(II) anion. *CrystEngComm* **2006**, *8*, 507–529.
71. Askarinejad, A.; Morsali, A. Potassium(I)thallium(I) heterometallic 3D polymeric mixed-anions compound, succinate-nitrate $[K_2Tl(MU-C_4H_4O_4)(MU-NO_3)]_n$. *Inorg. Chim. Acta* **2006**, *359*, 3379–3383.
72. Nagasubramanian, S.; Jayamani, A.; Thamilarasan, V.; Aravindan, G.; Ganesan, V.; Sengottuvelan, N. Hetero-metallic trigonal cage-shaped dimeric Ni_3K core complex of L-proline ligand: Synthesis, structural, electrochemical and DNA binding and cleavage activities. *J. Chem. Sci.* **2014**, *126*, 771–781.
73. Robin, M.B.; Day, P. Mixed Valence Chemistry-A Survey and Classification. *Adv. Inorg. Chem. Radiochem.* **1967**, *10*, 247–422.